# Styryl-N-phenyl-N'-(2-chloroethyl)ureas and Styrylphenylimidazolidin-2-ones as New Potent Microtubule-Disrupting Agents Using Combretastatin A-4 as Model

**ARTICLE** *in* EUROPEAN JOURNAL OF MEDICINAL CHEMISTRY · MAY 2015

Impact Factor: 3.45 · DOI: 10.1016/j.ejmech.2015.05.034



**6 AUTHORS**, INCLUDING:

Sébastien Fortin

Laval University

**29** PUBLICATIONS **251** CITATIONS

SEE PROFILE

Rene C.-Gaudreault

Centre Hospitalier Universitaire de Québec …

**103** PUBLICATIONS **1,301** CITATIONS

SEE PROFILE

European Journal of Medicinal Chemistry 100 (2015) 34–43

Contents lists available at ScienceDirect

European Journal of Medicinal Chemistry

journal homepage: http://www.elsevier.com/locate/ejmech

Short communication

# Styryl-*N*-phenyl-*N*′-(2-chloroethyl)ureas and styrylphenylimidazolidin-2-ones as new potent microtubule-disrupting agents using combretastatin A-4 as model

Mathieu Gagné-Boulet [a, 1], Sébastien Fortin [a, b, *, 1], Jacques Lacroix [a], Carole-Anne Lefebvre [a, 2], Marie-France Côté [a], René C.-Gaudreault [a, c, *]

[a] Centre de recherche du CHU de Québec, axe oncologie, Hôpital Saint-François d'Assise, Québec, QC G1L 3L5, Canada
[b] Faculté de pharmacie, Université Laval, Pavillon Vandry, Québec, QC G1V 0A6, Canada
[c] Faculté de médecine, Département de médecine moléculaire, Université Laval, Pavillon Vandry, Québec, QC G1V 0A6, Canada

ARTICLE INFO

*Article history:*
Received 7 April 2015
Received in revised form
21 May 2015
Accepted 22 May 2015
Available online 28 May 2015

*Keywords:*
Styrylphenylimidazolidin-2-ones
Styryl-*N*-phenyl-N′-(2-chloroethyl)ureas
Styryl-*N*-phenyl-*N*′-ethylureas
Combretastatin A-4
Colchicine-binding site inhibitors
Antimitotics

ABSTRACT

Combretastatin A-4 (CA-4) is a well-studied and attractive molecular template to develop new antimitotics. Several thousand of modifications were performed on the ring B and the ethenyl bridge of CA-4 but only a few involved the trimethoxyphenyl moiety (TMP, ring A) often considered essential to the antiproliferative and antimicrotubule activities. In this study, we described the design, the preparation, the characterization and the biological evaluation of three new series of CA-4 analogs namely styryl-*N*-phenyl-*N*′-ethylureas (SEUs), styryl-*N*-phenyl-*N*′-(2-chloroethyl)ureas (SCEUs) and styrylphenylimidazolidin-2-ones (SIMZs) bearing a 3-Cl (series **a**), 3,5-Me (series **b**) and TMP (series **c**) substituents, respectively. All SCEU and SIMZ *Z*-isomers were active in the high and the low nanomolar range, respectively. Conversely to SEUs and their *E*-isomers that were significantly less active or inactive. Interestingly, the TMP moiety is giving rise to derivatives exhibiting the lowest antiproliferative activity in the SCEU series (**10c**) and the most active compound in the SIMZ series (**12c**). Moreover, SIMZ *Z*-isomers bearing either a 3-Cl (**12a**) or a 3,5-Me (**12b**) exhibited antiproliferative activities that are also in the same order of magnitude as **12c**. All SCEU and SIMZ *Z*-isomers also arrested the cell cycle progression in G2/M phase, bound to the colchicine-binding site and disrupted the cytoskeleton of cancer cells. In addition to the promising and innovative microtubule-disrupting properties of SCEUs and SIMZs, these results show that the TMP moiety is not essential for the cytocidal activity of these new CA-4 analogs.


## 1. Introduction

Microtubules are heterodimers composed of α- and β-tubulin isoforms present in all eukaryotic cells. Microtubules are not only involved in cell shape but also in numerous cellular mechanisms such as cell motility and division mitosis, intracellular vesicle transport, organization, and positioning of membranous organelles [1]. When natural or synthetic ligands such as combretastatin A-4 (CA-4, **1**), podophyllotoxin (**2**) and phenstatin (**3**, Fig. 1) interact with microtubule dynamics, they disrupt the cytoskeleton, block mitosis into the G2/M phase and initiate an apoptotic program [2]. It is why molecules acting on the cellular microtubule dynamics form one of the largest groups of effective chemotherapeutics used against cancers. However, the efficacy and the clinical usefulness of currently available antimicrotubule agents are impeded by the occurrence of chemoresistance, systemic toxicity, and poor

*Abbreviations:* CA-4, combretastatin A-4; CAM assay, chorioallantoic membrane assay; C-BS, colchicine-binding site; CEU, *N*-phenyl-*N*′-(2-chloroethyl)urea; EBI, *N*,*N*′-ethylene-bis(iodoacetamide); EU, *N*-phenyl-*N*′-ethylurea; IMZ, phenylimidazolidin-2-one; PIB-SA, phenyl 4-(2-oxoimidazolidin-1-yl)benzenesulfonamide; PIB-SO, phenyl 4-(2-oxoimidazolidin-1-yl)benzenesulfonate; SAR, structure-activity relationships; SCEU, styryl-*N*-phenyl-*N*′-(2-chloroethyl)urea; SEU, styryl-*N*-phenyl-*N*′-ethylurea; SIMZ, styrylphenylimidazolidin-2-one; TMP, trimethoxyphenyl.

* Corresponding authors. Centre de recherche du CHU de Québec, axe oncologie, Hôpital Saint-François d'Assise, Québec, QC G1L 3L5, Canada.
*E-mail addresses:* sebastien.fortin@pha.ulaval.ca (S. Fortin), rene.c-gaudreault@crchudequebec.ulaval.ca (R. C.-Gaudreault).
[1] These authors contributed equally.
[2] Present address: Département de chimie, Université Laval, Pavillon Vachon, Québec, QC, Canada G1V 0A6.

http://dx.doi.org/10.1016/j.ejmech.2015.05.034
0223-5234/

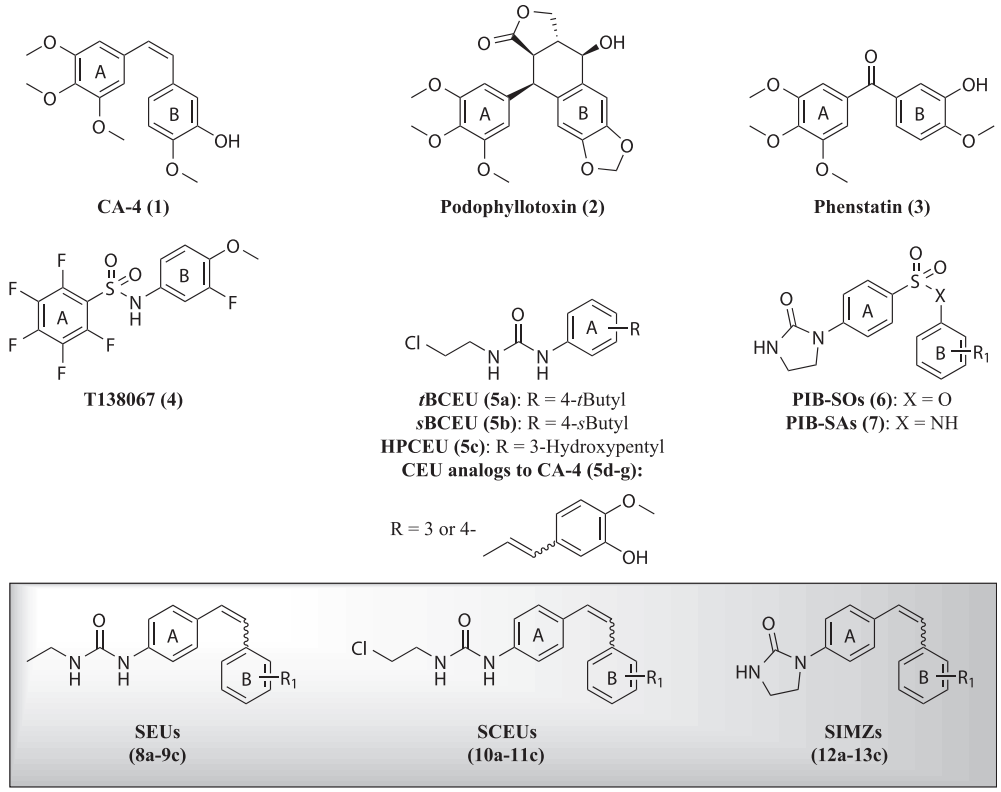


**Fig. 1.** Molecular structure of antimicrotubule agents: combretastatin A-4 (CA-4, **1**), podophyllotoxin (**2**), phenstatin (**3**), T138067 (**4**), *t*BCEU (**5a**), *s*BCEU (**5b**), HPCEU (**5c**), CEU analogs to CA-4 (**5d**–**g**), phenyl 4-(2-oxoimidazolidin-1-yl)benzenesulfonates (PIB–SOs, **6**), phenyl 4-(2-oxoimidazolidin-1-yl)benzenesulfonamides (PIB–SAs, **7**), styryl-*N*-phenyl-*N*′-ethylureas (SEUs **8a**–**9c**), styryl-*N*-phenyl-*N*′-(2-chloroethyl)ureas (SCEUs **10a**–**11c**) and styrylphenylimidazolidin-2-ones (SIMZs **12a**–**13c**).

biopharmaceutical properties [3,4]. Therefore, the search for new antimicrotubule agents exhibiting improved biopharmaceutical profiles and pharmacodynamics is still recognized as of utmost importance. To that end, tens of thousands of derivatives and analogs based on modifications of the ring B and the ethenyl bridge of CA-4 were synthesized and screened for anticancer activity [5,6]. However, only a few modifications were made on the trimethoxyphenyl (TMP) moiety (ring A, Fig. 1) of CA-4, notably its replacement by either a pentafluorophenyl (T138067, **4**) [7], a trimethylphenyl or a dimethylphenyl moiety [8]. Indeed, the TMP moiety presents in CA-4 and in numerous other antimicrotubule agents has long been considered as essential to their binding to the colchicine-binding site (C-BS), their inhibition of the microtubule assembly and their antiproliferative activity [9].

Based on the computational models published by Nogales [10] and others [11,12] we have designed and developed an *N*-phenyl-*N*′-(2-chloroethyl)urea (CEU) fragment that can be used as a "bioisosteric equivalent" of TMP that acylates the C-BS on the glutamic acid residue in position 198 [13,14]. This CEU fragment was used to prepare several antimicrotubule agents substituted at position 4 of the aromatic ring such as 1-(4-(*tert*-butyl)phenyl)-3-(2-chloroethyl)urea (*t*BCEU, **5a**) [15] and 1-(4-(*sec*-butyl)phenyl)-3-(2-chloroethyl)urea (*s*BCEU, **5b**) [15], and substituted at position 3 of the aromatic ring represented by 1-(2-chloroethyl)-3-(4-(5-hydroxypentyl)phenyl)urea (**5c**) [16]. This was also confirmed by replacing the TMP moiety of CA-4 by the CEU group resulting in molecules referred to as (*Z*)-1-(2-chloroethyl)-3-(4-(3-hydroxy-4-methoxystyryl)phenyl)ureas (CEU analogs to CA-4, **5d**–**g**, Fig. 1) exhibiting antiproliferative activity ($IC_{50}$) at the micromolar level and that are still acylating the C-BS [14,17]. Of note, only the methoxylated phenolic moieties of CA-4 at positions 3 and 4 have been studied so far. Recently our structure-activity relationship (SAR) studies showed that the modification of the ethenyl bridge by its sulfonate or sulfonamide bioisosteric equivalents followed by the cyclisation of the CEU moiety into the corresponding phenylimidazolidin-2-ones (IMZs) lead to potent new classes of antimicrotubule agents designated as phenyl 4-(2-oxoimidazolidin-1-yl)benzenesulfonates (PIB–SOs, **6**) [18] and phenyl 4-(2-oxoimidazolidin-1-yl)benzenesulfonamides (PIB–SAs, **7**) [19]. Compounds **6** and **7** exhibited antiproliferative activity in the nanomolar range similarly to CA-4, which represents an increase by up to 3 logs in magnitude of the antiproliferative activity when compared to compounds **5a**–**g**. Compounds **6** and **7** exhibited also high potency against human fibrosarcoma HT-1080 tumors grafted onto the chorioallantoic membrane of developing chick embryos (CAM assay) and low toxicity to the embryos. The SAR studies of these compounds showed that the nature of the bridge linking the 2 phenyl groups and the substituent on ring B of compounds **6** and **7** had a significant impact on the biological activity. Due to their molecular similarity, we hypothesized that the IMZ moiety of PIB-SOs and PIB-SAs is a "bioisosteric equivalent" of the TMP ring of CA-4 as is the CEU moiety. However, our recent molecular modeling experiments show that the IMZ moiety group might be docked in the C-BS in such way that it would mimic the tropolone and the methoxylated phenolic moieties of colchicine and CA-4, respectively instead the TPM moiety [20]. This might be due to the steric hindrance that may prevent the binding of the IMZ moiety to the adjacent pocket behind CYS239 and 354 residues of β-tubulin [20,21].

Based on these premises, we hypothesized that the sulfonate and the sulfonamide bridges of PIB-SO and PIB-SA analogs are bioisoteric equivalents of the ethenyl bridge. Moreover, we

postulated that the TMP moiety is not essential for the antiproliferative activity and the affinity for the C-BS. Finally, we postulated also that the chloro group and the methoxylated phenolic moieties are not optimal and essential for the activity of the CEU analogs of CA-4. To validate our hypothesis, we designed, prepared and biologically evaluated three series of CA-4 analogs named styryl-*N*-phenyl-*N*′-ethylureas (SEUs, **8** and **9**), styryl-*N*-phenyl-*N*′-(2-chloroethyl)ureas (SCEUs, **10** and **11**) and styrylphenylimidazolidin-2-ones (SIMZs, **12** and **13**) each one comprising the *E*- and *Z*-isomers. The substituents on the aromatic ring B namely, 3-Cl (series **a**) and 3,5-Me (series **b**) were selected for their potent antiproliferative activity in the PIB-SOs and PIB-SAs series and their dissimilarity providing a maximum of information for the SAR studies. The TMP moiety (series **c**) was selected to evaluate its importance on the antiproliferative and antimicrotubule activities on these new CA-4 analogs. These compounds were assessed for their antiproliferative activity on human cancer cell lines namely, HT-29, M21, MCF7 and HT-1080. Finally, the most potent compounds were assessed for their effect on cell cycle progression, cytoskeleton disruption and affinity to the C-BS.

## 2. Chemistry

**As shown in Scheme 1**, the general synthesis of SEUs, SCEUs and SIMZs started from triphenylphosphonium bromide salts (**14**) which were prepared by addition of triphenyphosphine to 4-nitrobenzyl bromides in toluene followed by the conjugation of 3-chlorobenzaldehyde, 3,5-dimethylbenzaldehyde or 3,4,5-trimethoxybenzaldehyde using the Wittig-coupling that was performed as described by Cushman et al. [22] and Fortin et al. [17]. Briefly, sodium hydride was added slowly to a stirring mixture of **14** and the relevant benzaldehyde in dry methylene chloride to yield **15a**–**c**. Afterward, the nitro group of compounds **15a**–**c** was reduced with iron dust and a catalytic amount of concentrated hydrochloric acid in a mixture of ethanol-water (10:1) into the corresponding *E*- and *Z*-amino stilbenes **16a**–**c** and **17a**–**c**. Of note, the *E*- and *Z*-isomers of series **b** were carefully separated at the conjugation step (compounds **15b**) while series **a** and **c** were separated at the reduction step (**16a**, **c** and **17a**, **c**). For the preparation of SEUs **8a**, **c** and **9a**, **c**, ethylisocyanate was added to the corresponding *E*- or *Z*-amino stilbenes **16a**, **c** and **17a**, **c** in methylene chloride at room temperature while SEUs **8b** and **9b** were prepared by addition of ethylisocyanate in acetonitrile at 90 °C under pressure. SCEUs **10a**–**11c** were obtained by addition of 2-chloroethylisocyanate to *E*- or *Z*-amino stilbenes **16a**–**17c** in methylene chloride at room temperature. Finally, SIMZs **12a**–**13c** were prepared by cyclisation of the CEU moiety of SCEUs **10a**–**11c** into IMZ in presence of sodium hydride in dry tetrahydrofuran.

## 3. Results/discussion

### 3.1. SCEUs and SIMZs exhibit antiproliferative activity on human tumor cell lines

First, SEUs (**8a**–**9c**), SCEUs (**10a**–**11c**) and SIMZs (**12a**–**13c**) were assessed for their antiproliferative activity on human colon carcinoma (HT-29), skin melanoma (M21), breast carcinoma (MCF7), and human fibrosarcoma (HT-1080) according to the NCI/NIH Developmental Therapeutics Program [23]. The results are summarized in Table 1 and expressed as the concentration of drug inhibiting cell growth by 50% ($IC_{50}$). SIMZs **12a**–**c** are active in the low nanomolar range (1.7–38 nM) and SCEUs **10a**–**c** are active at 130–1,400 nM while SEUs are either inactive or several logs less active than CA-4 analogs (11,000 to > 20,000 nM). As expected, the antiproliferative activity of the stilbene *Z*-isomers was up to 3 logs higher than their respective stilbene *E*-isomers similarly as observed with CA-4 derivatives and analogs. These SAR studies confirm several important elements for the activity and the design

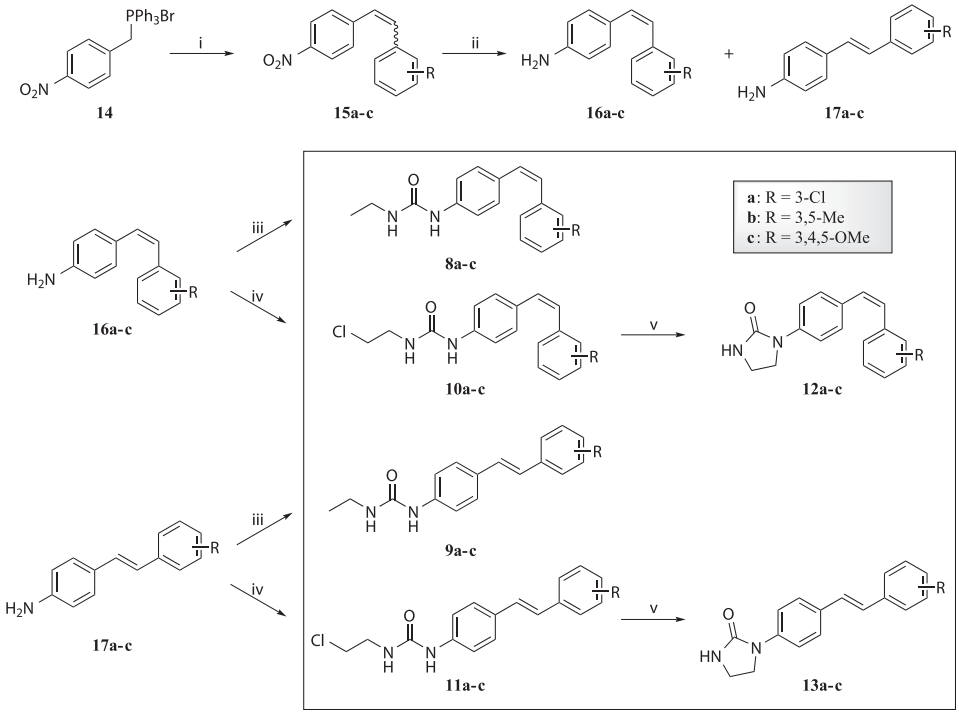


**Scheme 1.** Reagents and conditions: (i) 3-chlorobenzaldehyde, 3,5-dimethylbenzaldehyde or 3,4,5-trimethoxybenzaldehyde, NaH, DCM, 0 °C to rt, 24 h; (ii) Fe dust, HCl, EtOH:$H_2O$ (10:1), reflux 4 h; (iii) i. ethylisocyanate, DCM, rt, 3–4 days or ii. ethylisocyanate, $CH_3CN$, 90 °C, 48 h; (iv) 2-chloroethylisocyanate, DCM, rt, 1–3 days and (v) NaH, THF, 0 °C to rt., 4 h.

**Table 1**
Tumor cell growth inhibition by SEUs (**8a**–**9c**), SCEUs (**10a**–**11c**) and SIMZs (**12a**–**13c**) on HT-29, M21, MCF7 and HT-1080 human cancer cell lines.

| Compd | Tumor cell lines $IC_{50}$ (nM)[a] | | | |
|---|---|---|---|---|
| | HT-29 | M21 | MCF7 | HT-1080 |
| **8a** | 26,000 | 35,000 | 32,000 | 31,000 |
| **8b** | 11,000 | 16,000 | 17,000 | 15,000 |
| **8c** | 21,000 | 21,000 | 21,000 | 29,000 |
| **9a** | >20,000 | >20,000 | >20,000 | >20,000 |
| **9b** | >20,000 | >20,000 | >20,000 | >20,000 |
| **9c** | 12,000 | 29,000 | 17,000 | 16,000 |
| **10a** | 130 | 170 | 200 | 170 |
| **10b** | 510 | 710 | 860 | 700 |
| **10c** | 680 | 950 | 1400 | 1400 |
| **11a** | 12,000 | >20,000 | >20,000 | >20,000 |
| **11b** | 11,000 | >20,000 | 19,000 | >20,000 |
| **11c** | 9,500 | >20,000 | >20,000 | >20,000 |
| **12a** | 25 | 27 | 38 | 35 |
| **12b** | 8.4 | 10 | 23 | 15 |
| **12c** | 1.7 | 2.4 | 2.6 | 2.3 |
| **13a** | 17,000 | 19,000 | 20,000 | >20,000 |
| **13b** | 14,000 | 17,000 | 16,000 | >20,000 |
| **13c** | 370 | 550 | 540 | 400 |
| **CA-4**[b] | 560 | 1.6 | 2.1 | 1.8 |

[a] $IC_{50}$: Concentration of the drug required to inhibit cell growth by 50%.
[b] Combretastatin A-4 (CA-4) was used as positive control.

of these new CA-4 analogs. First, our studies show that the *Z*-ethenyl bridge is a bioisoteric equivalent of the sulfonate and the sulfonamide moieties. Indeed, this modification globally increases by approximately two-fold the activity of SIMZs comparatively to PIB-SO and PIB-SA analogs bearing the same substituents. These results strongly suggest and corroborate our molecular models showing that the sulfonate and the sulfonamide groups in PIB-SO and PIB-SA analogs must adopt a cisoid conformation to be active. Interestingly, the antiproliferative activities of SIMZs **12a**–**c** are in the low nanomolar range and are very similar to CA-4. In addition, they are at least 10-times more potent on HT-29 cells than CA-4. Moreover, although that SIMZ **12c** bearing a TMP moiety is the most active compound (1.7–2.6 nM), SIMZs bearing a 3-Cl (compound **12a**, 25–38 nM) or a 3,5-Me substituents (compound **12b**, 8.4–23 nM) are also in the same order of magnitude. This suggests that the TMP group is not essential for the antiproliferative activity of SIMZ derivatives. The antiproliferative activity of SIMZs increases in the following order of substitution of ring B: 3,4,5-OMe > 3,5-Me > 3-Cl.

The modification of the IMZ group by a CEU group lead to SCEUs that are active in the mid to high nanomolar range. On one hand, SCEUs are among the most potent CEUs prepared so far. Their antiproliferative activity is approximately 10-times higher than CEUs substituted at position 4 (e.g. **5a**, **b** and **d**) and in the same order of magnitude as CEUs substituted at position 3 (e.g. compound **5c**). They are approximately 2 to 10-times more active than CEU analogs to CA-4 that is bearing a methoxylated phenolic group. Moreover, SCEU **10c** bearing a 3-Cl substituent is the most potent CEU prepared to date and it exhibits an antiproliferative activity ranging between 130 and 200 nM. In addition, compounds **10b** and

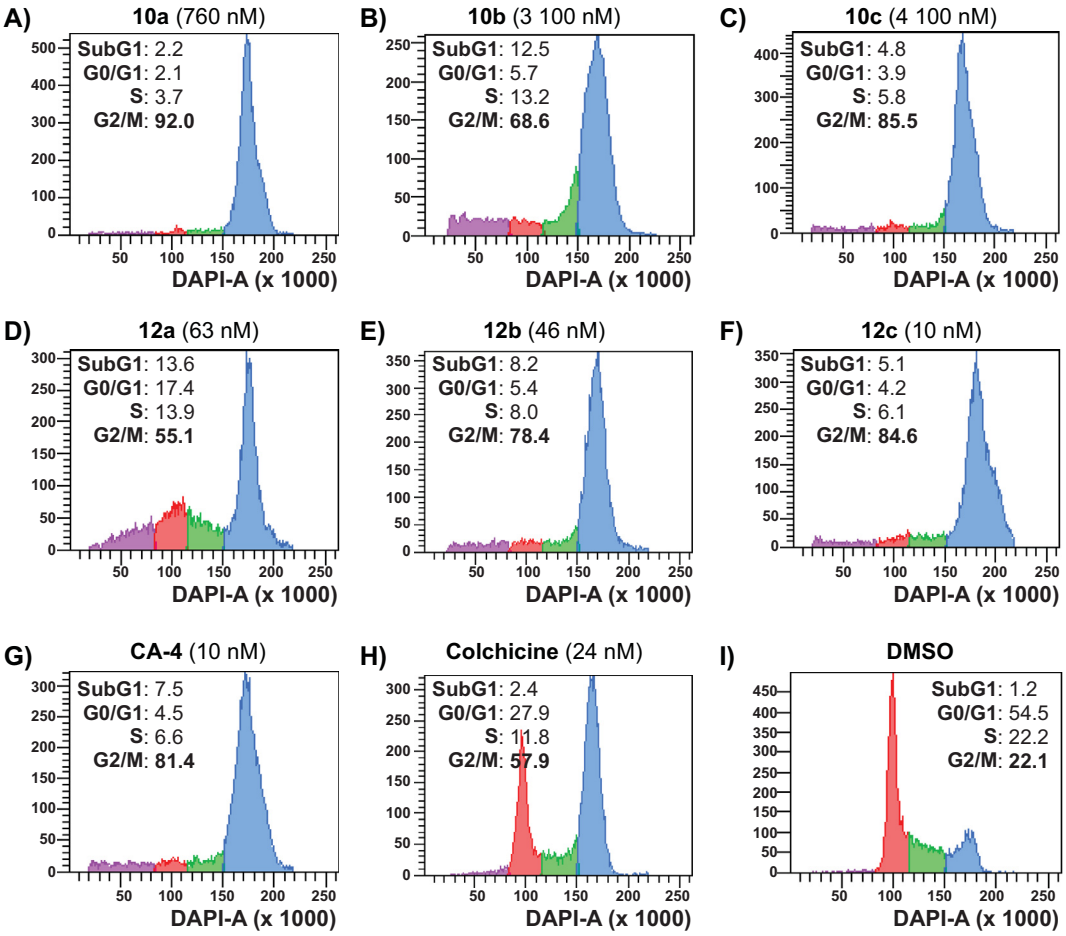


**Fig. 2.** Effect of SCEUs **10a**–**c** and SIMZs **12a**–**c** on cell cycle progression of M21 cells after 24 h of treatment. A) **10a**, B) **10b**, C) **10c**, D) **12a**, E) **12b**, F) **12c**. G) Combretastatin A-4 (CA-4) and H) colchicine were used as positive controls while **I)** DMSO was used as negative control.

**10c** are almost as potent as CA-4 on HT-29 cells. However, SCEUs are approximately 100-times less active than SIMZs. SAR studies show that the chloro group in the CEU moiety is essential for the antiproliferative activity; SEU derivatives without the chloro group are significantly less active or inactive even to those bearing a TMP moiety (compound **8c**, 21,000 to 29,000 nM). Moreover, the antiproliferative activity of SCEUs increases according to the following order of substitution of ring B: 3-Cl > 3,5-Me > 3,4,5-OMe which are in the opposite direction of SIMZs. These results confirm that the TMP group is not essential for the antiproliferative activity of these CA-4 analogs comparatively to the electrophilic chlorine atom presents in CEUs.

### 3.2. SCEUs and SIMZs arrest the cell cycle progression in $G_2$/M phase

The cell growth inhibitory potency of SCEUs (**10a**–**c**) and SIMZs **12a**–**c** prompted us to evaluate their effect on cell cycle progression and on the microtubules and cytoskeleton integrity on M21 cells. For cell cycle progression analysis, M21 cancer cells were treated at approximately 5-times the respective $IC_{50}$ of SCEUs and SIMZs for 24 h. As shown in Fig. 2, SCEUs **10a**–**c** and SIMZs **12a**–**c** arrested efficiently the cell cycle progression in G2/M phase; increasing the percentage of cells in G2/M phase by 33–70%. These results are comparable to CA-4 and colchicine used as positive controls that increase the percentage of cells in G2/M phase by 59 and 36%, respectively.

### 3.3. SCEUs and SIMZs disrupt the cytoskeleton of cancer cells

In the aim to assess the effect of SCEUs **10a**–**c** and SIMZs **12a**–**c** on microtubules and cytoskeleton integrity, M21 cells were treated for 24 h with **10a**–**c** and **12a**–**c** at 5-times their respective $IC_{50}$, and cellular microtubule structures were visualized by indirect immunofluorescence using an anti-β-tubulin monoclonal antibody. As shown in Fig. 3, **10a**–**c** and **12a**–**c** lead to microtubule depolymerization and cytoskeleton disruption on M21 cancer cells similarly to CA-4 and colchicine.

### 3.4. SCEUs acylate the glutamic acid residue in position 198 of the C-BS

We finally assessed whether the binding of SCEUs and SIMZs on β-tubulin was the same as CA-4 and colchicine that bind to the C-BS. As mentioned earlier, CEUs such as *t*BCEU [24] and *s*BCEU [25] are acylating the glutamic acid residue in position 198 of the C-BS [13,14]. This adduct is easily detectable by Western blot as a second immunoreacting band of β-tubulin [16,21,26–29]. As seen in Fig. 4, SCEUs **10a** and **10b** induce a significant second immunoreacting band at 1,500 and 3,100 nM, respectively while SCEUs **10c** bearing a TMP moiety induces only a very week second immunoreacting band at 8200 nM. These results confirm that SCEUs act on the C-BS and acylate the glutamic acid 198 residue of β-tubulin. These results also show that the TMP moiety is not essential for the affinity and the acylation of the C-BS. The weak antiproliferative activity and

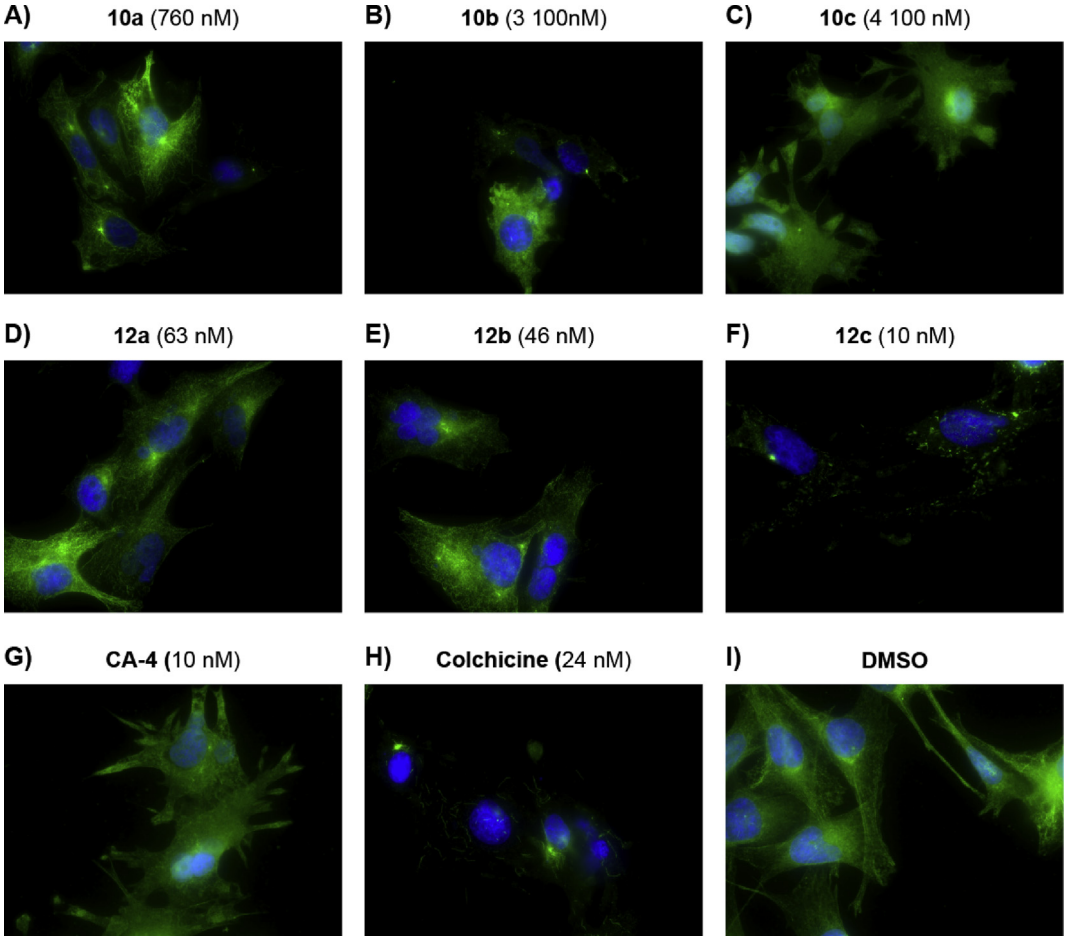


**Fig. 3.** Effect of **10a**–**c** and **12a**–**c** on the cytoskeleton integrity of M21 cells after 24 h of treatment. A) **10a**, B) **10b**, C) **10c**, D) **12a**, E) **12b**, F) **12c**. G) Combretastatin A-4 (CA-4) and H) colchicine were used as positive controls while I) DMSO was used as negative control.

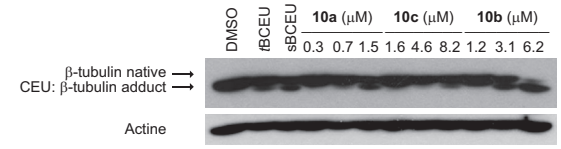


**Fig. 4.** Dose-dependent effect of SCEUs on the electrophoretic mobility shift assay of a covalently bound drug to β-tubulin. SCEUs **10a**, **10b** and **10c** were used at 2-, 5- and 10-times their respective $IC_{50}$. *t*BCEU (30 000 nM) and *s*BCEU (30 000 nM) were used as positive controls and DMSO as negative control.

the poor acylation of β-tubulin by SCEUs bearing a TMP group (compound **10c**) may be explained by the high affinity of the TMP for the hydrophobic pocket where is located the cysteine 239 residue disfavoring the conformation for an acylation by the glutamic acid at position 198.

### 3.5. SIMZs inhibit EBI binding to the C-BS

We recently develop a quick and simple detection technique to assess the binding of antimicrotubule agents that do not acylate/alkylate the C-BS such as SIMZs [30]. This assay is based on *N*,*N*′-ethylene-bis(iodoacetamide) (EBI) that has the ability to crosslink the cysteine residues at position 239 and 354 in the C-BS. Similarly to CEUs, EBI forms an adduct easily detectable by Western blot as a second immunoreacting band of β-tubulin. Antimicrotubule agents acting in the C-BS prevent the formation of the EBI: β-tubulin adduct. Briefly, M21 cells were treated with SIMZs **12a**, **12b**, **12c** at 100-times their respective $IC_{50}$ as well as SIMZ **13c** at 100,000 nM; the maximum concentration used for this assay. Colchicine at 10, 100, 1,000 and 10,000 nM was used as positive controls. As shown in Fig. 5, SIMZs **12a**, **12b**, **12c** and **13c** inhibit the formation of the EBI: β-tubulin adduct similarly to colchicine as shown by the disappearance of the second immunoreacting band of β-tubulin and the appearance of the native β-tubulin band (first immunoreacting band of β-tubulin). Interestingly, the experiment also shows that a large concentration of *E*-isomer of SIMZ bearing a trimethoxyl group (compound **13c**, approximately 100-times less potent than the *Z*-isomer SIMZ) inhibits also the formation of the EBI: β-tubulin adduct. First, these results show that IMZ and TMP groups have a significant affinity for the C-BS and explains the antiproliferative activity of SIMZ **13c** (370–550 nM) and the disruption of the cytoskeleton; *E*-isomers are usually weak or inactive compounds exhibiting in parallel only a weak affinity for the C-BS. Moreover, they show that the TMP group is not essential for the affinity of SIMZs to C-BS.

## 4. Conclusions

In summary, our studies identified new cytocidal molecules designed as SIMZs and SCEUs that are active in the low and high nanomolar ranges, respectively, as their parent compounds. They block the cell cycle progression in the G2/M phase, bind to the C-BS leading to the depolymerization of microtubules and disruption of the cytoskeleton. In addition, this study shows that the sulfonate and sulfonate bridges are bioisosteric equivalents of the ethenyl bridge of CA-4. Moreover, it shows that the TMP group is not essential for the antiproliferative and the antimicrotbule activities of SIMZs and SCEUs. Furthermore, SCEUs are among the most potent CEUs prepared so far and are 2 to 10-times more potent than CEU analogs to CA-4. Finally, SIMZs and SCEUs are new molecular scaffolds to design new potent antimicrotubule agents and could be used as alternative to circumvent some biopharmaceutical problems that might be encountered during the clinical development of CA-4.

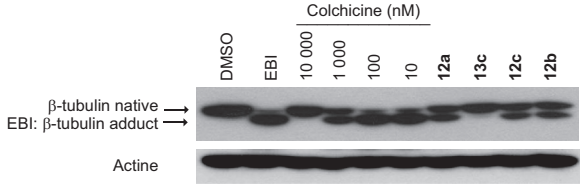


**Fig. 5.** Effect of SIMZs on the binding of EBI to the colchicine-binding site. SIMZ **12a** (410 nM), **12b** (910 nM), **12c** (2500 nM), **13c** (100 000 nM) were used approximately at 100-times their respective $IC_{50}$. Colchicine at 10, 100, 1 000, 10 000 nM were used as positive controls, DMSO as negative control and EBI as reference control.

## 5. Experimental protocols

### 5.1. Biological methods

#### 5.1.1. Cell lines culture

HT-29 human colon carcinoma, MCF7 human breast carcinoma, HT-1080 human fibrosarcoma were purchased from the American Type Culture Collection (Manassas, VA). M21 human skin melanoma cells were kindly provided by Dr. David Cheresh (University of California, San Diego School of Medicine, USA). Cells were cultured in DMEM medium containing sodium bicarbonate, high glucose concentration, glutamine and sodium pyruvate (Hyclone, Logan, UT) supplemented with 5% of fetal bovine serum (FBS, Invitrogen, Burlington, ON) and were maintained at 37 °C in a moisture-saturated atmosphere containing 5% $CO_2$.

#### 5.1.2. Antiproliferative activity assay

The antiproliferative activity assay of all compounds was assessed using the procedure recommended by the National Cancer Institute for its drug screening program with slight modifications [23]. Briefly, 96-well microtiter plates were seeded with 75 μL of a suspension of HT-29 ($4.0 \times 10^3$), M21 ($3.0 \times 10^3$), MCF7 ($2.5 \times 10^3$) or HT-1080 ($2.5 \times 10^3$) cells per well in DMEM and incubated for 24 h. Drugs freshly solubilized in DMSO were diluted in fresh DMEM, and 75 μL aliquots containing serially diluted concentrations of the drug were added. Final drug concentrations ranged from 50 μM to 1 nM. DMSO was maintained at a concentration of <0.5% (v/v) to avoid any related cytotoxicity. Plates were incubated for 48 h. Afterward, cell growth was stopped by addition of cold trichloroacetic acid to the wells (10% w/v, final concentration), followed by a 1 h incubation at 4 °C. Plates were then washed 5-times with water. Then, 75 μL of a sulforhodamine B solution (0.1% w/v) in 1% acetic acid was added to each well, and the plates were incubated for 15 min at room temperature. After staining, unbound dye was removed by washing 5-times with 1% acetic acid. Bound dye was solubilized in 20 mM Tris base, and the absorbance was read using an optimal wavelength (530–568 nm) with a μQuant Universal microplate spectrophotometer (Biotek, Winooski, VT). Readings obtained from treated cells were compared with measurements from control cell plates fixed on treatment day, and the percentage of cell growth inhibition was calculated for each drug. The experiments were performed at least twice in triplicate. The assays were considered valid when the coefficient of variation for a given set of conditions and within the same experiment was <10%.

#### 5.1.3. Cell cycle analysis

After incubation of $2.5 \times 10^5$ M21 cells with the drugs at 2- and 5-times their respective $IC_{50}$, for 24 h, the cells were trypsinized, washed with Phosphate Buffered Saline (PBS) and resuspended in

250 μL of PBS. Cells were fixed by the addition of 750 μL of ice-cold EtOH under agitation and stored at −20 °C until analysis. Prior to fluorescence-activated cell sorting analysis, cells were washed with PBS and resuspended in 500 μL of PBS containing 2 μg/mL DAPI. Cell cycle distribution of fixed cell suspensions was analyzed using an LSR II flow cytometer (BD Biosciences, Franklin Lakes, NJ).

*5.1.4. Immunofluorescence*

Cover slides (22 mm × 22 mm) sterilized with 70% (v/v) EtOH were placed in six-well plates. To promote cell adhesion, cover slides were treated with 1.5 mL of a fibronectin solution in PBS (5 μg/mL) for 1 h at 37 °C. Slides were then rinsed twice with PBS. M21 cells ($1 \times 10^5$) were seeded onto the plates and incubated for 24 h. Cells were then incubated with the compound to be tested at 2- and 5-times their respective $IC_{50}$ for 24 h. The control solution was DMSO diluted in the culture medium (0.5%, v/v). Cells were fixed using 1 mL of formaldehyde at 3.7% and permeabilized by addition of a saponin solution (0.1% in PBS) containing 3% (w/v) BSA (saponin-BSA). Cells were incubated with mouse anti-β-tubulin antibody (clone TUB 2.1, 1/200) (Sigma-Aldrich, St. Louis, MO) in saponin-BSA. Cover slides were next incubated for 2 h at room temperature and then washed twice with PBS supplemented with 0.05% (v/v) Tween 20 (PBST). Saponin-BSA containing goat anti-mouse IgG conjugated to AlexaFluor 594 (1/1000, Invitrogen, Burlington, Ontario, Canada), and DAPI (0.3 μg/mL, Sigma, Oakville, Ontario, Canada) was then added. The cover slides were incubated for 1 h at room temperature and then washed twice with PBST and twice with PBS. The cover slides were mounted with Fluorescence Mounting Medium (Burlington, Ontario, Canada). Cells were visualized using an epifluorescence microscope (Olympus BX51, Center Valley, PA) with a Qimaging RETIGA EXi camera (Qimaging, Surrey, British Columbia, Canada).

*5.1.5. β-tubulin acylation assay*

M21 cells ($4.0 \times 10^5$) were plated in 6-well plates and incubated overnight. The cells were treated for 24 h at 2, 5 and 10-times the respective $IC_{50}$ for SCEUs, at 30,000 nM of CEU-022 and CEU-071 (used as positive controls) and at 0.5% of DMSO (used as negative control).

*5.1.6. Competition and inhibition of EBI binding to β-tubulin*

M21 cells ($7.5 \times 10^5$) were plated in 6-well plates and incubated overnight. The cells were treated for 1.5 h at 100-times the $IC_{50}$ for SIMZs (cutoff at 100,000 nM for **13a**) and at 10, 100, 1,000 and 10,000 nM for colchicine. Then, 100 μL of EBI (Toronto Research Chemicals, North York, Ontario, Canada) in PBS (100 μM, final concentration) were then added for 1.5 h without changing the culture medium, which contains the drug tested.

*5.1.7. Gel electrophoresis and immunoblot*

For both assays, after incubation of the cells with the drugs, the supernatant was collected and the cells were trypsinized (trypsine-EDTA 0.5%), harvested and centrifuged for 5 min at 12,000 rpm. The pellets were washed with 500 μL of cold PBS and stored at −80 °C until use. The cells pellets were resuspended in buffer (0.32 M sucrose, 1 mM EDTA at pH 8, 10 mM Tris at pH 7.4 and protease inhibitor).

The protein concentration was determined using the Bio-Rad protein assay (Bio-Rad laboratories, Mississauga, Canada). Samples were prepared to obtain protein at a concentration of 2 mg/ml in Laemmli [31] sample (60 mM Tris-Cl at pH 6.8, 2% SDS, 10% glycerol, 5% β-mercaptoethanol, 0.01% bromophenol blue) and boiled for 5 min. Forty micrograms of proteins from the protein extracts were subjected to electrophoresis using 10% polyacrylamide gels. The proteins were transferred onto nitrocellulose membranes that were incubated with TBSTM (Tris-Buffered Saline + 0.1% (v/v) Tween-20 with 5% fat-free dry milk) for 2 h at room temperature, and then with the anti-β-tubulin (clone TUB 2.1) (Sigma–Aldrich, St. Louis, MO) primary antibody in TBSTM (1:500) for 2 h at room temperature. Membranes were washed with TBST (Tris-Buffered Saline with +0.1% (v/v) Tween 20) and incubated with peroxidase conjugated anti-mouse immunoglobulin (Amersham Canada, Oakville, Canada) in TBSMT (1:5000) for 1 h at room temperature. After washing the membranes with TBST, detection of the immunoblot was carried out using Clarity Western enhanced chemiluminescence reagents (Bio-Rad laboratories, Mississauga, Canada). Detection of bands was performed with Super Rx medical X-Ray film (Fujifilm, Tokyo Japan).

*5.2. Chemical methods*

*5.2.1. General*

Proton NMR spectra were recorded on a Bruker AM-300 spectrometer (Bruker, Germany). Chemical shifts (δ) are reported in parts per million. Uncorrected melting points were determined on an electrothermal melting point apparatus. HPLC analyses were performed using a Prominence LCMS-2020 system with binary solvent equipped with a UV/vis photodiode array and an APCI probe (Shimadzu, Columbia, MD). Compounds were eluted within 23 min on an Alltech Alltima C18 reversed-phase column (5 μm, 250 mm × 4.6 mm) equipped with an Alltech Alltima C18 pre-column (5 μm, 7.5 mm × 4.6 mm) with a MeOH/$H_2O$ linear gradient at 1.0 mL/min. Purity of the final compounds was >95%. All reactions were performed under a dried Ar atmosphere. All chemicals were supplied by Sigma–Aldrich Canada (Oakville, Ontario, Canada) or VWR International (Mont-Royal, Québec, Canada) and used as received unless specified otherwise. Liquid flash chromatography was performed on silica gel F60, 60A, 40–63 μm supplied by Silicycle (Quebec, Canada) using an FPX flash purification system (Biotage, Charlottesville, VA) and using solvent mixtures expressed as v/v ratios. Solvents and reagents were used without purification unless specified otherwise. The progress of the reactions was monitored by TLC using precoated silica gel 60 F254 TLC plates (VWR International, Ville Mont-Royal, Québec). The chromatograms were viewed under UV light at 254 and/or 265 nm.

*5.2.2. General preparation of compounds **8a–c** and **9a–c***

*5.2.2.1. Method A.* Ethyl isocyanate (1.2–2 Eq) was added to a solution of the appropriate aniline (**16a**, **c** and **17a**, **c**, 1 Eq) in methylene chloride (15 mL). The reaction mixture was stirred at room temperature for 3–5 days. The solvent was evaporated under reduced pressure, and the compound was purified by flash chromatography using a mixture of hexane/ethyl acetate.

*5.2.2.2. Method B.* Ethyl isocyanate (3 Eq) was added to the appropriate aniline (**16b** and **17b**, 1 Eq) dissolved in acetonitrile (2 mL). The reaction mixture was heated to 90 °C in a sealed tube and stirred for 48 h. Afterward, the mixture was cooled to room temperature, $SiO_2$ was added and the solvent evaporated to dryness under reduced pressure. The residue adsorbed on $SiO_2$ was purified by flash chromatography on silica gel using a mixture of hexane/ethyl acetate.

*5.2.3. Characterization of compounds **8a–c** and **9a–c***

*5.2.3.1. (Z)-1-(4-(3-Chlorostyryl)phenyl)-3-ethylurea (**8a**).* Method A, flash chromatography (hexane/ethyl acetate (75:25)). Yield: 57%; fade yellow solid; mp: 121–123 °C; $^1$H RMN (DMSO-$d_6$): δ 8.50 (s, 1H, NH), 7.31–7.19 (m, 6H, Ar), 7.09 (d, 2H, $J$ = 8.6 Hz, Ar), 6.61 (d, 1H, $J$ = 12.2 Hz, CH), 6.48 (d, 1H, $J$ = 12.2 Hz, CH), 6.13 (t, 1H, $J$ = 5.4 Hz, NH), 3.14–3.10 (m, 2H, $J$ = 7.1 Hz, $CH_2$), 1.05 (t, 3H,

$J$ = 7.1 Hz, $CH_3$); $^{13}C$ NMR (DMSO-$d_6$): δ 155.0, 140.1, 139.5, 133.0, 131.3, 130.2, 129.1, 128.7, 128.1, 127.1, 126.9, 126.7, 117.3, 34.0, 15.4; MS (ES+) found 301.10; $C_{17}H_{17}ClN_2O$ ($M^+$ + H) requires 301.11.

*5.2.3.2. (Z)-1-(4-(3,5-Dimethylstyryl)phenyl)-3-ethylurea (**8b**).* Method B, flash chromatography (1. hexane to hexane/ethyl acetate (65:35) and 2. methylene chloride to methylene chloride/ethyl acetate (90:10)). Yield: 81%; white solid; mp: 147–149 °C; $^1H$ RMN ($CDCl_3$): δ 7.20 (d, 2H, $J$ = 8.7 Hz, Ar), 7.12 (d, 2H, $J$ = 8.5 Hz, Ar), 6.89 (s, 2H, Ar), 6.84 (s, 1H, Ar), 6.52–6.42 (m, 2H, CH), 3.27 (q, 2H, $J$ = 7.2 Hz, $CH_2$), 2.22 (s, 6H, $CH_3$), 1.12 (t, 3H, $J$ = 7.2 Hz, $CH_3$); $^{13}C$ NMR ($CDCl_3$): 155.8, 137.7, 137.4, 137.3, 132.9, 129.9, 129.1, 128.8, 126.5, 120.5, 35.2, 21.2, 15.4; MS (ES+) found 295.15; $C_{19}H_{22}N_2O$ ($M^+$ + H) requires 295.18.

*5.2.3.3. (Z)-1-Ethyl-3-(4-(3,4,5-trimethoxystyryl)phenyl)urea (**8c**).* Method A, flash chromatography (hexane/ethyl acetate (75:25)). Yield: 21%; brown-orange solid; mp: 104–106 °C; $^1H$ RMN ($CDCl_3$): δ 7.23–7.17 (m, 4H, Ar), 7.09 (s, 1H, NH), 6.50–6.47 (m, 3H, Ar and CH), 6.42 (d, 1H, $J$ = 12.3 Hz, CH), 5.26 (t, 1H, $J$ = 5.4 Hz, NH), 3.84 (s, 3H, $CH_3$), 3.67 (s, 6H, $CH_3$), 3.28–3.19 (m, 2H, $CH_2$), 1.10 (t, 3H, $J$ = 7.2 Hz, $CH_3$); $^{13}C$ NMR ($CDCl_3$): δ 155.8, 152.9, 138.3, 136.7, 133.1, 131.7, 129.8, 129.6, 129.1, 119.3, 105.9, 61.0, 55.9, 35.0, 15.4; MS (ES+) found 357.20; $C_{20}H_{24}N_2O_4$ ($M^+$ + H) requires 357.18.

*5.2.3.4. (E)-1-(4-(3-Chlorostyryl)phenyl)-3-ethylurea (**9a**).* Method A, flash chromatography (hexane/ethyl acetate (75:25)). Yield: 49%; fade orange solid; mp: 208–210 °C; $^1H$ RMN (DMSO-$d_6$): δ 8.58 (s, 1H, NH), 7.66 (s, 1H, Ar), 7.54–7.37 (m, 6H, Ar), 7.30–7.25 (m, 2H, Ar and CH), 7.09 (d, 1H, $J$ = 16.2 Hz, CH), 6.16 (t, 1H, $J$ = 5.3 Hz, NH), 3.15–3.08 (m, 2H, $CH_2$), 1.07 (t, 3H, $J$ = 7.2 Hz, $CH_3$); $^{13}C$ NMR (DMSO-$d_6$): δ 155.0, 140.7, 139.9, 133.6, 130.5, 130.1, 129.4, 127.3, 126.7, 125.6, 124.8, 124.2, 117.6, 34.0, 15.5; MS (ES+) found 301.10; $C_{17}H_{17}ClN_2O$ ($M^+$ + H) requires 301.11.

*5.2.3.5. (E)-1-(4-(3,5-Dimethylstyryl)phenyl)-3-ethylurea (**9b**).* Method B, flash chromatography (1. hexane to hexane/ethyl acetate (65:35) and 2. methylene chloride to methylene chloride/ethyl acetate (90:10)). Yield: 50%; white solid; mp: 216–217 °C; $^1H$ RMN ($CDCl_3$ and MeOD): δ 7.12 (d, 2H, $J$ = 8.6 Hz, Ar), 7.05 (d, 2H, $J$ = 8.7 Hz, Ar), 6.82 (s, 2H, Ar), 6.75 (d, 1H, $J$ = 15 Hz, CH), 6.64 (d, 1H, $J$ = 16.3 Hz, CH), 6.58 (s, 1H, Ar), 2.96 (q, 2H, $J$ = 7.3 Hz, $CH_2$), 2.03 (s, 6H, $CH_2$), 0.87 (t, 3H, $J$ = 7.3 Hz, $CH_3$); $^{13}C$ NMR ($CDCl_3$ and MeOD): δ 156.4, 138.6, 137.6, 137.1, 131.4, 128.6, 127.4, 126.6, 126.5, 123.7, 118.6, 34.2, 20.5, 14.5; MS (ES+) found 295.18; $C_{19}H_{22}N_2O$ ($M^+$ + H) requires 295.18.

*5.2.3.6. (E)-1-Ethyl-3-(4-(3,4,5-trimethoxystyryl)phenyl)urea (**9c**).* Method A, flash chromatography (methylene chloride/ethyl acetate (85:15)). Yield: 69%; white solid; mp: 185–187 °C; $^1H$ RMN (DMSO-$d_6$): δ 7.36 (d, 2H, $J$ = 8.6 Hz, Ar), 7.30 (d, 2H, $J$ = 8.6 Hz, Ar), 6.92 (m, 2H, CH), 6.66 (s, 2H, Ar), 3.85 (s, 6H, $CH_3$), 3.82 (s, 3H, $CH_3$), 3.21 (q, 2H, $J$ = 7.2 Hz, $CH_2$), 1.09 (t, 3H, $J$ = 7.3 Hz, $CH_3$); $^{13}C$ NMR ($CDCl_3$ and MeOD): δ 156.2, 153.3, 138.9, 137.4, 133.5, 131.6, 127.9, 127.1, 126.8, 119.5, 119.4, 103.3, 61.0, 56.0, 34.9, 34.7, 15.3; MS (ES+) found 357.20; $C_{20}H_{24}N_2O_4$ ($M^+$ + H) requires 357.18.

*5.2.4. General preparation of compounds **10a–c** and **11a–c***

2-Chloroethyl isocyanate (1.2 Eq) was added to a solution of the appropriate aniline (**16a–c** and **17a–c**, 1 Eq) in methylene chloride (15 mL). The reaction mixture was stirred at room temperature for 1–3 days. The solvent was evaporated under reduced pressure, and the compound was purified by flash chromatography.

*5.2.5. Characterization of compounds **10a–c** and **11a–c***

*5.2.5.1. (Z)-1-(2-Chloroethyl)-3-(4-(3-chlorostyryl)phenyl)urea (**10a**).* Flash chromatography (methylene chloride/ethyl acetate (75:25)). Yield: 75%; white solid; mp: 100–102 °C; $^1H$ RMN (DMSO-$d_6$): δ 8.75 (s, 1H, NH), 7.33–7.20 (m, 6H, Ar), 7.10 (d, 2H, $J$ = 8.5 Hz, Ar), 6.62 (d, 1H, $J$ = 12.2 Hz, CH), 6.50 (d, 1H, $J$ = 12.2 Hz, CH), 6.45 (t, 1H, $J$ = 5.7 Hz, NH), 3.66 (t, 2H, $J$ = 6.1 Hz, $CH_2$), 3.45–3.41 (m, 2H, $CH_2$); $^{13}C$ NMR (DMSO-$d_6$): δ 154.9, 139.8, 139.5, 133.0, 131.3, 130.2, 129.1, 129.0, 128.1, 127.1, 126.9, 126.8, 117.4, 44.4, 41.2; MS (ES+) found 335.10; $C_{17}H_{16}Cl_2N_2O$ ($M^+$ + H) requires 335.07.

*5.2.5.2. (Z)-1-(2-Chloroethyl)-3-(4-(3,5-dimethylstyryl)phenyl)urea (**10b**).* Flash chromatography (methylene chloride/methanol (96:4)). Yield: 87%; white solid; mp: 103–105 °C; $^1H$ RMN ($CDCl_3$): δ 7.22 (d, 2H, $J$ = 8.5 Hz, Ar), 7.14, (d, 2H, $J$ = 8.6 Hz, Ar), 6.89–6.75 (m, 4H, Ar and NH), 6.51 (d, 1H, $J$ = 12.4 Hz, CH), 6.45 (d, 1H, $J$ = 11.4 Hz, CH), 5.43 (br, 1H, NH), 3.63–3.58 (m, 4H, $CH_2$), 2.22 (s, 6H, $CH_3$); $^{13}C$ NMR ($CDCl_3$): δ 155.5, 137.8, 137.3, 136.9, 133.2, 130.1, 130.0, 129.0, 128.8, 126.5, 120.7, 44.8, 42.1, 21.3; MS (ES+) found 329.15; $C_{19}H_{21}ClN_2O$ ($M^+$ + H) requires 329.14.

*5.2.5.3. (Z)-1-(2-Chloroethyl)-3-(4-(3,4,5-trimethoxystyryl)phenyl) urea (**10c**).* Flash chromatography (methylene chloride/ethyl acetate (90:10)). Yield: 41%; dark red solid; mp: 67–69 °C; $^1H$ RMN ($CDCl_3$): δ 7.82 (s, 1H, NH), 7.22 (d, 2H, $J$ = 8.7 Hz, Ar), 7.16 (d, 2H, $J$ = 8.6 Hz, Ar), 6.50 (s, 2H, Ar), 6.47 (d, 1H, $J$ = 12.5 Hz, CH), 6.40 (d, 1H, $J$ = 12.2 Hz, CH), 6.11 (t, 1H, $J$ = 5.6 Hz, NH), 3.83 (s, 3H, $CH_3$), 3.65 (s, 6H, $CH_3$), 3.56–3.49 (m, 4H, $CH_2$); $^{13}C$ NMR ($CDCl_3$): δ 156.0, 152.8, 138.3, 136.6, 133.2, 131.6, 129.7, 129.7, 129.0, 118.9, 105.9, 61.0, 55.9, 44.4, 41.9; MS (ES+) found 391.15; $C_{20}H_{23}ClN_2O_4$ ($M^+$ + H) requires 391.14.

*5.2.5.4. (E)-1-(2-Chloroethyl)-3-(4-(3-chlorostyryl)phenyl)urea (**11a**).* Flash chromatography (methylene chloride/ethyl acetate (90:10)). Yield: 97%; fade yellow solid; mp: 192–193 °C; $^1H$ RMN (DMSO-$d_6$): δ 8.81 (s, 1H, NH), 7.65–7.25 (m, 9H, Ar and CH), 7.10 (d, 1H, $J$ = 16.4 Hz, CH), 6.47 (t, 1H, $J$ = 5.7 Hz, NH), 3.68 (t, 2H, $J$ = 6.2 Hz, $CH_2$), 3.47–3.41 (m, 2H, $CH_2$); $^{13}C$ NMR (DMSO-$d_6$): δ 154.9, 140.4, 139.9, 133.6, 130.5, 130.0, 129.8, 127.3, 126.8, 125.6, 124.9, 124.5, 117.8, 44.4, 41.3; MS (ES+) found 335.10; $C_{17}H_{16}Cl_2N_2O$ ($M^+$ + H) requires 335.07.

*5.2.5.5. (E)-1-(2-Chloroethyl)-3-(4-(3,5-dimethylstyryl)phenyl)urea (**11b**).* Flash chromatography (hexane/ethyl acetate (75:25)). Yield: 59%; white solid; mp: 194–195 °C; $^1H$ RMN (DMSO-$d_6$): δ 8.78 (s, 1H, NH), 7.47 (d, 2H, $J$ = 8.5 Hz, Ar), 7.42 (d, 2H, $J$ = 8.4 Hz, Ar), 7.18–7.11 (m, 3H, Ar and CH), 7.01 (d, 1H, $J$ = 16.4 Hz, CH), 6.89 (s, 1H, Ar), 6.46 (t, 1H, $J$ = 5.5 Hz, NH), 3.68 (t, 2H, $J$ = 5.9 Hz, $CH_2$), 3.47–3.41 (m, 2H, $CH_2$), 2.29 (s, 6H, $CH_3$); $^{13}C$ NMR (DMSO-$d_6$): δ 155.0, 139.9, 137.6, 137.3, 130.3, 128.8, 127.9, 127.0, 126.1, 124.1, 117.8, 44.5, 41.2, 21.0; MS (ES+) found 329.15; $C_{19}H_{21}ClN_2O$ ($M^+$ + H) requires 329.14.

*5.2.5.6. (E)-1-(2-Chloroethyl)-3-(4-(3,4,5-trimethoxystyryl)phenyl) urea (**11c**).* Flash chromatography (methylene chloride/ethyl acetate (90:10)). Yield: 68%; white solid; mp: 161–163 °C; $^1H$ RMN ($CDCl_3$): δ 7.98 (s, 1H, NH), 7.38 (d, 2H, $J$ = 8.6 Hz, Ar), 7.32 (d, 2H, $J$ = 8.5 Hz, Ar), 6.94 (d, 1H, $J$ = 16.6 Hz, CH), 6.88 (d, 1H, $J$ = 16.4 Hz, CH), 6.68 (s, 2H, Ar), 6.24 (t, 1H, $J$ = 5.7 Hz, NH), 3.87 (br, 9H, $CH_3$), 3.62–3.52 (m, 4H, $CH_2$); $^{13}C$ NMR ($CDCl_3$): δ 156.3, 153.3, 138.6, 137.3, 133.6, 132.0, 127.8, 127.2, 119.9, 103.3, 61.1, 56.1, 44.3, 42.0; MS (ES+) found 391.15; $C_{20}H_{23}ClN_2O_4$ ($M^+$ + H) requires 391.14.

*5.2.6. General preparation of compounds **12a–c** and **13a–c***

Sodium hydride (3 Eq) was added slowly to a cold solution of 2-

chloroethylurea derivative (compounds **10a**–**c** and **11a**–**c**, 1 Eq) in dry tetrahydrofuran under Ar atmosphere. The ice bath was then removed after 30 min and the reaction mixture was stirred at room temperature for 4 h. Excess of sodium hydride was quenched by the addition of water (20 mL) at 0 °C. Tetrahydrofuran from the reaction mixture was evaporated under reduced pressure. The aqueous phase was extracted thrice by methylene chloride (20 mL). The combined organic phases were washed with brine (40 mL), dried over anhydrous sodium sulfate, filtered, and evaporated to dryness under vacuum. The residue was purified by flash chromatography on silica gel.

*5.2.7. Characterization of compounds **12a**–**c** and **13a**–**c***

*5.2.7.1. (Z)-1-(4-(3-Chlorostyryl)phenyl)imidazolidin-2-one (**12a**).* Flash chromatography (hexane/ethyl acetate (75:25)). Yield: 85%; white sticky solid; $^1$H RMN (DMSO-$d_6$): δ 7.48 (d, 2H, $J$ = 8.7 Hz, Ar), 7.32–7.15 (m, 6H, Ar), 7.01 (s, 1H, NH), 6.65 (d, 1H, $J$ = 12.2 Hz, CH), 6.53 (d, 1H, $J$ = 12.2 Hz, CH), 3.84 (t, 2H, $J$ = 7.4 Hz, $CH_2$), 3.43–3.31 (m, 2H, $CH_2$ hidden by the water peak); $^{13}$C NMR (DMSO-$d_6$): δ 158.9, 140.2, 139.5, 133.1, 131.1, 130.3, 129.1, 128.9, 128.1, 127.1, 127.0, 116.5, 44.3, 36.5; MS (ES+) found 299.10; $C_{17}H_{15}ClN_2O$ ($M^+$ + H) requires 299.10.

*5.2.7.2. (Z)-1-(4-(3,5-Dimethylstyryl)phenyl)imidazolidin-2-one (**12b**).* Flash chromatography (methylene chloride to methylene chloride/ethyl acetate (75:25)). Yield: 99%; white solid; mp: 169–171 °C; $^1$H RMN ($CDCl_3$ and MeOH): δ 7.35 (d, 2H, $J$ = 9.2 Hz, Ar), 7.22 (d, 2H, $J$ = 8.7 Hz, Ar), 6.89 (s, 2H, Ar), 6.84 (s, 1H, Ar), 6.48 (s, 2H, CH), 3.91 (t, 2H, $J$ = 6.0 Hz, $CH_2$), 3.53 (t, 2H, $J$ = 8.7 Hz, $CH_2$), 2.22 (s, 6H, $CH_3$); $^{13}$C NMR ($CDCl_3$): δ 160.1, 138.4, 137.1, 137.0, 131.3, 129.0, 128.8, 128.7, 128.0, 125.9, 117.0, 44.9, 36.7, 20.2; MS (ES+) found 293.15; $C_{19}H_{20}N_2O$ ($M^+$ + H) requires 293.17.

*5.2.7.3. (Z)-1-(4-(3,4,5-Trimethoxystyryl)phenyl)imidazolidin-2-one (**12c**).* Flash chromatography (methylene chloride to methylene chloride/ethyl acetate (50/50)). Yield: 49%; yellow oil; $^1$H RMN ($CDCl_3$): δ 7.40 (d, 2H, $J$ = 7.8 Hz, Ar), 7.25 (d, 2H, $J$ = 8.0 Hz, Ar), 6.49–6.40 (m, 4H, Ar and CH), 6.11 (s, 1H, NH), 3.87–3.82 (m, 5H, $CH_2$ and $CH_3$), 3.66 (s, 6H, $CH_3$), 3.52 (t, 2H, $J$ = 7.6 Hz, $CH_2$); $^{13}$C NMR ($CDCl_3$): δ 160.1, 152.9, 139.2, 137.1, 132.9, 131.2, 129.5, 129.2, 117.2, 105.9, 60.9, 56.0, 45.2, 37.5; MS (ES+) found 355.15; $C_{20}H_{22}N_2O_4$ ($M^+$ + H) requires 355.17.

*5.2.7.4. (E)-1-(4-(3-Chlorostyryl)phenyl)imidazolidin-2-one (**13a**).* Flash chromatography (hexane/ethyl acetate (75:25)). Yield: 97%; white solid; mp: 249–251 °C; $^1$H RMN (DMSO-$d_6$): δ 7.68 (br, 1H, NH), 7.62–7.53 (m, 5H, Ar), 7.42–7.29 (m, 3H, Ar), 7.17–7.06 (m, 2H, CH), 3.89 (t, 2H, $J$ = 7.3 Hz, $CH_2$), 3.43 (t, 2H, $J$ = 8.0 Hz, $CH_2$); $^{13}$C NMR (DMSO-$d_6$): δ 158.9, 140.7, 139.8, 133.6, 130.5, 129.9, 129.9, 127.1, 126.8, 125.7, 124.9, 124.8, 116.9, 44.4, 36.6; MS (ES+) found 299.10; $C_{17}H_{15}ClN_2O$ ($M^+$ + H) requires 299.10.

*5.2.7.5. (E)-1-(4-(3,5-Dimethylstyryl)phenyl)imidazolidin-2-one (**13b**).* Flash chromatography (methylene chloride to methylene chloride/ethyl acetate (75:25)). Yield: 95%; white solid; mp: 207–209 °C; $^1$H RMN (DMSO-$d_6$): δ 7.58 (d, 2H, $J$ = 8.9 Hz, Ar), 7.53 (d, 2H, $J$ = 8.9 Hz, Ar), 7.19–7.01 (m, 5H, Ar and CH), 6.89 (br, 1H, NH), 3.91–3.85 (m, 2H, $CH_2$), 3.45–3.40 (m, 2H, $CH_2$), 2.30 (s, 6H, $CH_3$); $^{13}$C NMR (DMSO-$d_6$): δ 158.9, 140.2, 137.6, 137.2, 130.4, 128.9, 127.8, 126.8, 126.5, 124.1, 117.0, 44.4, 36.6, 21.0; MS (ES+) found 293.15; $C_{19}H_{20}N_2O$ ($M^+$ + H) requires 293.17.

*5.2.7.6. (E)-1-(4-(3,4,5-Trimethoxystyryl)phenyl)imidazolidin-2-one (**13c**).* Flash chromatography (methylene chloride/ethyl acetate (50:50)). Yield: 99%; white solid; mp: 157–159 °C; $^1$H RMN ($CDCl_3$): δ 7.54 (d, 2H, $J$ = 8.8 Hz, Ar), 7.48 (d, 2H, $J$ = 8.8 Hz, Ar), 7.02–6.91 (m, 2H, CH), 6.73 (s, 2H, Ar), 5.40 (br, 1H, NH), 3.97–3.92 (m, 8H, $CH_2$ and $CH_3$), 3.87 (s, 3H, $CH_3$), 3.58 (t, 2H, $J$ = 8.3 Hz, $CH_2$); $^{13}$C NMR ($CDCl_3$): δ 159.7, 153.4, 139.6, 137.7, 133.3, 131.6, 127.7, 127.3, 127.0, 117.9, 103.4, 61.0, 56.1, 45.3, 37.5; MS (ES+) found 355.15; $C_{20}H_{22}N_2O_4$ ($M^+$ + H) requires 355.17.

*5.2.8. General preparation of compounds **15a**–**c***

Compounds **15a**–**c** were synthesized using the methods described by Cushman [22] and Fortin [17]. First, compound **14** was prepared according to the procedure of Fortin et al. [17]. Briefly, triphenyphosphine (1.0 Eq, 13.9 mmol) was added to a solution of 4-nitrobenzyl bromides (1.0 Eq, 13.9 mmol) in toluene (60 mL) and heated to reflux for 12 h. The mixture was then cooled at room temperature and the precipitate was filtrate and triturate with toluene to give a white solid in quantitative yield. Afterwards, sodium hydride (3 Eq, 12.5 mmol) was added portion-wise to a well-stirred suspension of 4-nitrobenzylphosphonium bromide **14** (2 Eq, 8.4 mmol) and a relevant benzaldehyde (2 Eq, 8.4 mmol) in methylene chloride (90 mL) under an argon atmosphere at 0 °C. Subsequently, the mixture was warmed to room temperature. After further stirring for 24 h, excess sodium hydride was quenched by the addition of water (20 mL) at 0 °C. The aqueous phase was extracted thrice by methylene chloride (20 mL). The combined organic phases were washed with brine (40 mL), dried over anhydrous sodium sulfate, filtered, and evaporated to dryness under vacuum. The residue was purified by flash chromatography on silica gel with a mixture of hexane/methylene chloride for **15a** and hexane/ethyl acetate for **15b**, **c**. The geometric isomers of compound **15b** (yield, Z-isomer 33% and E-isomer 50%) were separated at this step whereas the geometric isomers of compounds **15a**, **c** were used as a mixture for the next chemical reaction (yield, 83% for **15a** and 98% for the **15c**).

*5.2.9. General preparation of compounds **16a**–**c** and **17a**–**c***

The appropriate nitro compound (1.0 Eq, 2.1 mmol) was dissolved in a mixture of EtOH and $H_2O$ (10:1, 60 mL). Powdered iron (7.3 Eq, 15.1 mmol) and a few drops of concentrated hydrochloric acid (8 drops) were added and the mixture was refluxed for 4 h. After cooling, the mixture was filtered on Celite® and rinsed with methylene chloride. Then, the ethanol and methylene chloride were evaporated and the aqueous phase was extracted thrice by methylene chloride (50 mL). The combined organic phases were washed with brine (60 mL), dried over anhydrous sodium sulfate, filtered, and evaporated to dryness under vacuum. The residue was purified by flash chromatography on silica gel using a mixture of hexane/methylene chloride for **16a** (yield: 20%) and **17a** (yield: 44%), hexane/ethyl acetate for **16b** (yield: 54%) and **17b** (yield: 72%), and methylene chloride/ethyl acetate for **16c** (yield: 26%) and **17c** (yield: 27%). All the geometric isomers were isolated at this step.

## Acknowledgment

This work was supported by a grant from the Canadian Health Research Institute (RCG, Grant #MOP-79334 and #MOP-89707).

## Appendix A. Supplementary data

Supplementary data related to this article can be found at http://dx.doi.org/10.1016/j.ejmech.2015.05.034.

## References

[1] P. Verdier-Pinard, F. Wang, R.H. Angeletti, S.B. Horwitz, G.A. Orr, The Role of Microtubules in Cell Biology, Neurobiology and Oncology, Humana press,

Totowa, NJ (USA), 2008.
[2] J.A. Ecsedy, M. Manfredi, A. Chakravarty, N. D'Amore, Current and next generation antimitotic therapies in cancer, in: D.A. Frank (Ed.), Signaling Pathways in Cancer Pathogenesis and Therapy, Springer Science + Business Media, 2012, p. 148.
[3] A.I. Minchinton, I.F. Tannock, Drug penetration in solid tumours, Nat. Rev. 6 (2006) 583–592.
[4] R. Grantab, S. Sivananthan, I.F. Tannock, The penetration of anticancer drugs through tumor tissue as a function of cellular adhesion and packing density of tumor cells, Cancer Res. 66 (2006) 1033–1039.
[5] Y. Shan, J. Zhang, Z. Liu, M. Wang, Y. Dong, Developments of combretastatin A-4 derivatives as anticancer agents, Curr. Med. Chem. 18 (2011) 523–538.
[6] Y. Lu, J.J. Chen, M. Xiao, W. Li, D.D. Miller, An overview of tubulin inhibitors that interact with the colchicine binding site, Pharm. Res.-Dordr 29 (2012) 2943–2971.
[7] B. Shan, J.C. Medina, E. Santha, W.P. Frankmoelle, T.C. Chou, R.M. Learned, M.R. Narbut, D. Stott, P. Wu, J.C. Jaen, T. Rosen, P.B. Timmermans, H. Beckmann, Selective, covalent modification of β-tubulin residue Cys-239 by T138067, an antitumor agent with in vivo efficacy against multidrug-resistant tumors, Proc. Natl. Acad. Sci. U S A. 96 (1999) 5686–5691.
[8] K. Gaukroger, J.A. Hadfield, N.J. Lawrence, S. Nolan, A.T. McGown, Structural requirements for the interaction of combretastatins with tubulin: how important is the trimethoxy unit? Org. Biomol. Chem. 1 (2003) 3033–3037.
[9] G.C. Tron, T. Pirali, G. Sorba, F. Pagliai, S. Busacca, A.A. Genazzani, Medicinal chemistry of combretastatin A4: present and future directions, J. Med. Chem. 49 (2006) 3033–3044.
[10] E. Nogales, Structural insight inte microtubule function, Annu. Rev. Biophys. Biomol. Struct. 30 (2001) 397–420.
[11] T.L. Nguyen, C. McGrath, A.R. Hermone, J.C. Burnett, D.W. Zaharevitz, B.W. Day, P. Wipf, E. Hamel, R. Gussio, A common pharmacophore for a diverse set of colchicine site inhibitors using a structure-based approach, J. Med. Chem. 48 (2005) 6107–6116.
[12] A. Dorleans, B. Gigant, R.B. Ravelli, P. Mailliet, V. Mikol, M. Knossow, Variations in the colchicine-binding domain provide insight into the structural switch of tubulin, Proc. Natl. Acad. Sci. U S A. 106 (2009) 13775–13779.
[13] B. Bouchon, C. Chambon, E. Mounetou, J. Papon, E. Miot-Noirault, R. C.-Gaudreault, J.-C. Madelmont, F. Degoul, Alkylation of β-tubulin on glu 198 by a microtubule disrupter, Mol. Pharmacol. 68 (2005) 1415–1422.
[14] S. Fortin, B. Bouchon, C. Chambon, J. Lacroix, E. Moreau, J.-M. Chezal, F. Degoul, R. C.-Gaudreault, Characterization of the covalent binding of *N*-phenyl-N′-(2-chloroethyl)ureas to β-tubulin: importance of glutamic acid 198 in microtubule stability, J. Pharmacol. Exp. Ther. 336 (2011) 460–467.
[15] P. Béchard, J. Lacroix, P. Poyet, R. C.-Gaudreault, Synthesis and cytotoxic activity of new alkyl[3-(2-chloroethyl)ureido]benzene derivatives, Eur. J. Med. Chem. 29 (1994) 963–966.
[16] E. Moreau, S. Fortin, M. Desjardins, J.L. Rousseau, E. Petitclerc, R. C.-Gaudreault, Optimized *N*-phenyl-N′-(2-chloroethyl)ureas as potential antineoplastic agents: synthesis and growth inhibition activity, Bioorg. Med. Chem. 13 (2005) 6703–6712.
[17] S. Fortin, E. Moreau, J. Lacroix, J.-C. Teulade, A. Patenaude, R. C.-Gaudreault, *N*-Phenyl-N′-(2-chloroethyl)urea analogues of combretastatin A-4: Is the *N*-phenyl-*N*′-(2-chloroethyl)urea pharmacophore mimicking the trimethoxy phenyl moiety? Bioorg. Med. Chem. Lett. 17 (2007) 2000–2004.
[18] S. Fortin, L. Wei, E. Moreau, J. Lacroix, M.-F. Côte, E. Petitclerc, L.P. Kotra, R. C.-Gaudreault, Design, synthesis, biological evaluation, and structure-activity relationships of substituted phenyl 4-(2-oxoimidazolidin-1-yl)benzenesulfonates as new tubulin inhibitors mimicking combretastatin A-4, J. Med. Chem. 54 (2011) 4559–4580.
[19] S. Fortin, L. Wei, E. Moreau, J. Lacroix, M.F. Cote, E. Petitclerc, L.P. Kotra, R. C.-Gaudreault, Substituted phenyl 4-(2-oxoimidazolidin-1-yl)benzenesulfonamides as antimitotics. Antiproliferative, antiangiogenic and antitumoral activity, and quantitative structure-activity relationships, Eur. J. Med. Chem. 46 (2011) 5327–5342.
[20] S. Fortin, L. Wei, L.P. Kotra, R. C.-Gaudreault, Novel cytocidal substituted phenyl 4-(2-oxoimidazolidin-1-yl) benzenesulfonates and benzenesulfonamides with affinity to the colchicine-binding site: is the phenyl 2-imidazolidinone moiety a new haptophore for the design of new antimitotics? Open J. Med. Chem. 5 (2015) 9–22.
[21] S. Fortin, L. Wei, E. Moreau, P. Labrie, E. Petitclerc, L.P. Kotra, R. C.-Gaudreault, Mechanism of action of *N*-phenyl-N′-(2-chloroethyl)ureas in the colchicine-binding site at the interface between α- and β-tubulin, Bioorg. Med. Chem. 17 (2009) 3690–3697.
[22] M. Cushman, D. Nagarathnam, D. Gopal, A.K. Chakraborti, C.M. Lin, E. Hamel, Synthesis and evaluation of stilbene and dihydrostilbene derivatives as potential anticancer agents that inhibit tubulin polymerization, J. Med. Chem. 34 (1991) 2579–2588.
[23] National Cancer Institute (NCI/NIH), Developmental therapeutics program human tumor cell line screen, URL : http://dtp.nci.nih.gov/branches/btb/ivclsp.html, (accessed 17.02.15).
[24] A. Patenaude, R.G. Deschesnes, J.L. Rousseau, E. Petitclerc, J. Lacroix, M.-F. Cote, R. C.-Gaudreault, New soft alkylating agents with enhanced cytotoxicity against cancer cells resistant to chemotherapeutics and hypoxia, Cancer Res. 67 (2007) 2306–2316.
[25] J. Legault, J.F. Gaulin, E. Mounetou, S. Bolduc, J. Lacroix, P. Poyet, R. C.-Gaudreault, Microtubule disruption induced *in vivo* by alkylation of β-tubulin by 1-aryl-3-(2-chloroethyl)ureas, a novel class of soft alkylating agents, Cancer Res. 60 (2000) 985–992.
[26] S. Fortin, P. Labrie, E. Moreau, L. Wei, L.P. Kotra, R. C.-Gaudreault, A comparative molecular field and comparative molecular similarity indices analyses (CoMFA and CoMSIA) of *N*-phenyl-*N*′-(2-chloroethyl)ureas targeting the colchicine-binding site as anticancer agents, Bioorg. Med. Chem. 16 (2008) 1914–1926.
[27] S. Fortin, E. Moreau, J. Lacroix, M.F. Cote, E. Petitclerc, R. C.-Gaudreault, Synthesis, antiproliferative activity evaluation and structure-activity relationships of novel aromatic urea and amide analogues of *N*-phenyl-N′-(2-chloroethyl) ureas, Eur. J. Med. Chem. 45 (2010) 2928–2937.
[28] S. Fortin, E. Moreau, A. Patenaude, M. Desjardins, J. Lacroix, J.L. Rousseau, R. C.-Gaudreault, *N*-Phenyl-*N*′-(2-chloroethyl)ureas (CEU) as potential antineoplastic agents. Part 2: role of ω-hydroxyl group in the covalent binding to β-tubulin, Bioorg. Med. Chem. 15 (2007) 1430–1438.
[29] E. Moreau, S. Fortin, J. Lacroix, A. Patenaude, J.L. Rousseau, R. C.-Gaudreault, *N*-Phenyl-*N*′-(2-chloroethyl)ureas (CEUs) as potential antineoplastic agents. Part 3: role of carbonyl groups in the covalent binding to the colchicine-binding site, Bioorg. Med. Chem. 16 (2008) 1206–1217.
[30] S. Fortin, J. Lacroix, M.F. Cote, E. Moreau, E. Petitclerc, R. C.-Gaudreault, Quick and simple detection technique to assess the binding of antimicrotubule agents to the colchicine-binding site, Biol. Proced. Online 12 (2010) 113–117.
[31] U.K. Laemmli, Cleavage of structural proteins during the assembly of the head of bacteriophage T4, Nature 227 (1970) 680–685.